Biogeosciences, 10, 2993–3005, 2013
www.biogeosciences.net/10/2993/2013/
doi:10.5194/bg-10-2993-2013

Biogeosciences Open Access

Net sea–air CO_2 flux uncertainties in the Bay of Biscay based on the choice of wind speed products and gas transfer parameterizations

P. Otero[1], X. A. Padin[2], M. Ruiz-Villarreal[1], L. M. García-García[1], A. F. Ríos[2], and F. F. Pérez[2]

[1]Instituto Español de Oceanografía, Centro Oceanográfico de A Coruña, Apdo. 130, 15080, A Coruña, Spain
[2]Instituto de Investigacións Mariñas, Consejo Superior de Investigaciones Científicas, c/ Eduardo Cabello 6, 36208, Vigo, Spain

Correspondence to: P. Otero (pablo.otero@co.ieo.es)

Received: 26 June 2012 – Published in Biogeosciences Discuss.: 1 August 2012
Revised: 22 November 2012 – Accepted: 14 April 2013 – Published: 3 May 2013

Abstract. The estimation of sea–air CO_2 fluxes is largely dependent on wind speed through the gas transfer velocity parameterization. In this paper, we quantify uncertainties in the estimation of the CO_2 uptake in the Bay of Biscay resulting from the use of different sources of wind speed such as three different global reanalysis meteorological models (NCEP/NCAR 1, NCEP/DOE 2 and ERA-Interim), one high-resolution regional forecast model (HIRLAM-AEMet), winds derived under the Cross-Calibrated Multi-Platform (CCMP) project, and QuikSCAT winds in combination with some of the most widely used gas transfer velocity parameterizations. Results show that net CO_2 flux estimations during an entire seasonal cycle (September 2002–September 2003) may vary by a factor of ~ 3 depending on the selected wind speed product and the gas exchange parameterization, with the highest impact due to the last one. The comparison of satellite- and model-derived winds with observations at buoys advises against the systematic overestimation of NCEP-2 and the underestimation of NCEP-1. In the coastal region, the presence of land and the time resolution are the main constraints of QuikSCAT, which turns CCMP and ERA-Interim in the preferred options.

1 Introduction

The CO_2 emissions associated with human activity are mainly due to the combustion of fossil fuels, gas flaring, cement production, land use changes and biomass burning (Solomon et al., 2007). After entering the atmosphere, CO_2 exchanges rapidly with the short-lived components of the terrestrial biosphere and surface ocean. The subsequent redistribution in long-term carbon reservoirs, including the deep ocean, mitigates in part the anthropogenic CO_2 emissions. The oceanic uptake fraction is estimated to be about one-third of this value (Sabine et al., 2004). Changes in the behavior of the oceans as atmospheric CO_2 catcher are, therefore, a key factor to predict future climate scenarios (Riebesell et al., 2009).

The accurate estimation of net CO_2 fluxes through the sea–air interface (FCO_2) is a priority for the marine carbon community, aimed at reducing uncertainties in the global carbon budget. The reliability of the inferred FCO_2 is intimately linked to the accuracy of the determinations of sea–air pCO_2 gradient (ΔpCO_2), the solubility of CO_2 (α) and the gas transfer – or piston – velocity (k). Thus, FCO_2 can be expressed as

$$FCO_2 = k \cdot \alpha \cdot \Delta pCO_2. \quad (1)$$

The determination of ΔpCO_2 is based on in situ measurements, being different international projects, such as the Global Carbon Project, leading the production of high quality and comparable datasets. The uncertainty in determining the solubility of CO_2, which depends on temperature and salinity, is relatively small (Weiss, 1974). Nowadays, most of the uncertainty in FCO_2 is attributed to the estimation of k (Takahashi et al., 2009), which is mainly parameterized as a function of the wind speed. This dependency highly differs among studies, and it has been stated as linear (e.g., Liss and Merlivat, 1986), quadratic (e.g., Wanninkhof, 1992; Nightingale et al., 2000; Sweeney et al., 2007) and

cubic (e.g., McGillis et al., 2001); other physical processes affect the estimation to a lesser extent, such as thermal stability (e.g., Erickson, 1993), the presence of surface surfactants (Tsai and Liu, 2003) and rainfall (Takagaki and Komori, 2007).

Due to the non-consensus with respect to the best k parameterization, special attention should also be paid to the quality of the wind speed data, which directly affects the piston velocity (Wanninkhof, 1992; Naegler et al., 2006), particularly using quadratic or cubic k parameterizations. The use of in situ measurements on ships is usually the preferred option; however, the airflow distortion at anemometer sites by the ship's hull and superstructure introduces biases (Griessbaum et al., 2010), which are difficult to quantify. This problem becomes especially relevant when observations are done using voluntary observing ships (VOSs), usually long cargo ships not designed with sampling purposes. Alternatively, records from meteorological buoys do not always coexist in space and time with ΔpCO_2 measurements. In these cases, model- or satellite-derived winds are the alternative because of the synoptic nature and the uniformity of the datasets, although they present intrinsic uncertainties. Model-derived winds, from both analysis and forecast, have broad coverage and high temporal resolution, and account for a recent improvement due to the assimilation of satellite observations (e.g., Chelton and Wentz, 2005). Despite these advances, most atmospheric models have been developed to provide weather forecast over land regions, and hence minor efforts have been done to prove their skill over the ocean and coastal regions (Otero and Ruiz-Villarreal, 2008). Differences among models are mainly related to the spatial resolution, data assimilation, boundary forcing, smoothing of the topography and parameterization of physical processes, especially those in the marine boundary layer. Satellite-derived winds are expected to provide top-quality results in most of the weather conditions. However, these estimations from remote sensors are affected by the presence of land in near-coastal regions and have a lower temporal resolution.

From above, it is easily deduced that the intrinsic nature of the wind products in combination with the different k parameterizations will produce a bunch of FCO_2 estimations. This effect was addressed in the global ocean (Boutin et al., 2002; Olsen et al., 2005; Naegler et al., 2006), although coastal regions (estuaries and continental shelves) were excluded from these FCO_2 sensitivity studies mainly due to the high spatial and temporal ΔpCO_2 variability of these environments (Laruelle et al., 2010). Coastal areas represent less than 8 % of the oceanic surface, but they support intense inputs of nutrients from land through rivers and significant horizontal carbon interchange with the open ocean, especially through break upwelling, which turn them into active biogeochemical areas. In spite of their key role in the carbon cycle, these regions were usually excluded from the budgets of sea–air CO_2 exchange at global scale (Sabine et al., 2004; Takahashi et al., 2009). Recent efforts have included them in the net CO_2 global budget (Chen and Borges, 2009; Laruelle et al., 2010), and have contributed to clarify the role of continental shelves as sinks of atmospheric CO_2 and near-shore ecosystems as sources of CO_2 to the atmosphere.

In this study, we will analyze the agreement between several wind products (observation-, model- and satellite-retrieved winds) available in the coastal region off northwest Iberia (Spain) and the Bay of Biscay, and the effect that the choice of one of these wind products in combination with several widely used k parameterizations has on the net FCO_2 estimations of this region. Since this area is characterized by a high uptake of anthropogenic atmospheric CO_2 (Gruber, 1998), it strongly contributes to the prime role that the North Atlantic Ocean plays in the global carbon cycle (Takahashi et al., 2009) and has profusely been described in numerous articles (Pérez et al., 1999; Borges and Frankignoulle, 2002; Padin et al., 2008; de la Paz et al., 2010). Moreover, different coastal environments such as estuaries, upwelling systems and open continental shelves unite in this marginal sea. Thus, the northern region is affected by the plume of the river Loire, the longest river in France – impacted by ~ 5 million inhabitants who live along its banks – whereas recurrent upwelling happens off NW Iberia, at the southern part of the study region. This fact allows us to study the effect of transfer velocity and wind speed product on net FCO_2 in terms of coastal typology. The main goal is to clarify the effect of wind speed products in our coastal sea, to identify suitable products for FCO_2 estimations, and to warn about discrepancies that would affect a bunch of published CO_2 studies in this coastal sea.

2 Data and methods

2.1 ΔpCO_2 measurements

The database was obtained in the Bay of Biscay using ships of opportunity (RORO *L'Audace* and *Surprise*) of the Suardíaz Company that regularly covered the route from Vigo, Spain, to St. Nazaire, France, and occasionally to Southampton, UK (Fig. 1). ECO (Evolution of CO_2 increase using ship of Opportunity: Galicia and Bay of Biscay) is the name of the project that involves measurements collected during these transects. A total of 75 journeys were performed from September 2002 to September 2003.

Mole fractions of CO_2 in air (xCO_2^{sw}) in equilibrium with a flowing stream of seawater (xCO_2^{sw}) pumped from 3 m below the surface, were recorded throughout each transit with a non-dispersive infrared gas analyzer (Li-6262, LI-COR) and used to derive ΔpCO_2 measurements. This analyzer was calibrated at the beginning and at the end of each transit using two gases: one of CO_2-free air and one of high CO_2 standard gases, which has a concentration of 375 ppm certified by Agencia Estatal de Meteorología (Canary Islands, Spain). xCO_2^{atm} was measured every hour by recording

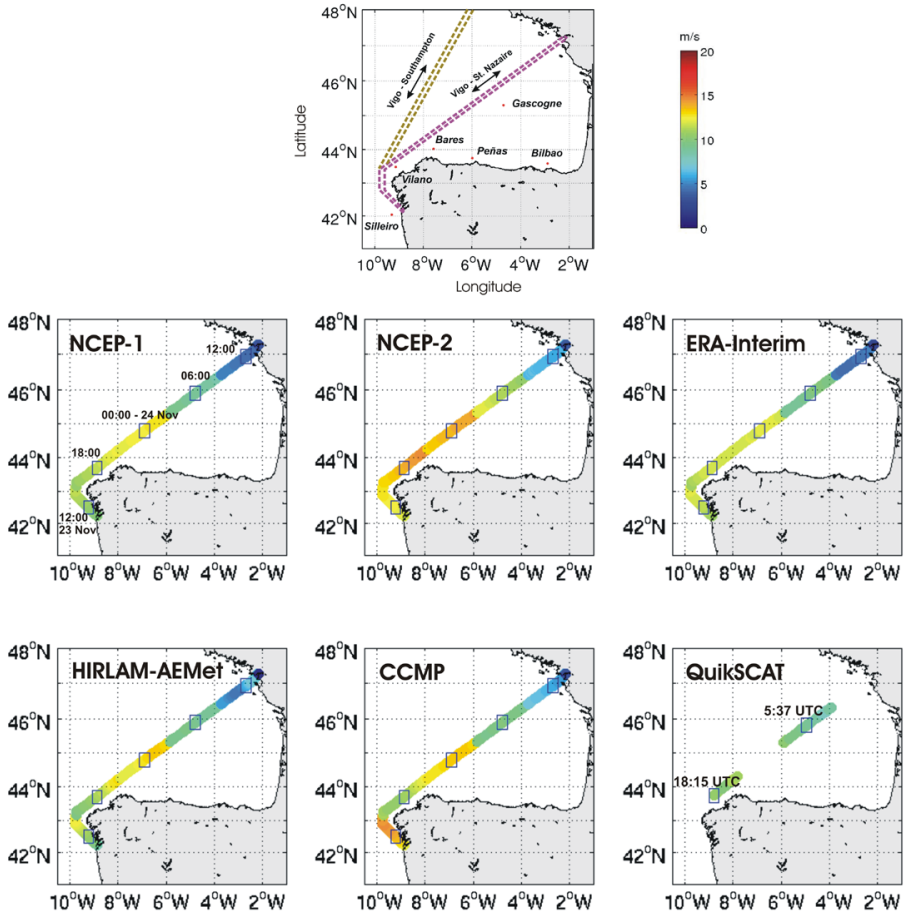

Fig. 1. Map of the Bay of Biscay showing ECO routes with ΔpCO_2 measures from September 2002 to September 2003 (top and left panel). These routes departed from the port of Vigo (Spain), usually to Saint Nazaire (France) and rarely to Southampton (UK). The ocean buoys used in the study (Silleiro, Vilano, Bares, Peñas, Bilbao and Gascogne) are also shown. The rest of the panels show the wind field interpolated in space (cubically in the case of models and collocated in satellite-derived winds) and time (< 3 h) to the first available route on 23 and 24 November 2002 as taken from different products (NCEP-1, NCEP-2, HIRLAM-AEMet, ERA-Interim, CCMP and QuikSCAT). The reference times of the wind products are marked over the route (blue boxes).

20 observations limited to a 5 min interval. A selection criterion was applied to eliminate spurious values and to identify xCO_2^{atm} representative data and, subsequently, fitted to a seasonal curve following Padin et al. (2007). xCO_2 was converted into pCO_2 using the atmospheric pressure as described in the DOE Handbook (1994), and corrected for the shift between in situ and equilibrator temperatures using an empirical equation proposed by Takahashi et al. (1993). Part of the pumped flowing stream passed through a thermosalinometer (SBE-45-MicroTSG) to record salinity and temperature values. A detailed description of these methods can be found in de la Paz et al. (2010).

2.2 Estimation of the sea–air FCO_2 flux

Sea–air FCO_2 is the result of multiplying the seawater solubility (Weiss, 1974), k and ΔpCO_2 (Eq. 1). In this paper, various of the most used expressions for k are evaluated: $k_{L\&M}$ (Liss and Merlivat, 1986) is a linear relationship, based on experiments in wind tunnels and measurements on lakes, with changing slope at different wind speed ranges, classified as smooth surface, rough surface and breaking waves regimes. k_W (Wanninkhof, 1992) is a quadratic relationship deduced from a fit to the Geochemical Ocean Sections Study (GEOSECS) bomb ^{14}C inventory (Broecker et al., 1985) for short-term wind speed. Both k_W and $k_{L\&M}$ are the most frequent parameterizations used in the FCO_2 estimations integrated in the global coastal balance. k_N (Nightingale et al., 2000) is included as a quadratic transfer velocity adequate for field studies on a local scale deduced from dual tracer experiments at sea. k_S (Sweeney et al., 2007) is a recent recalculation of transfer velocity from the ocean inventory of bomb-produced ^{14}C computed using NCEP-1 winds. Finally, k_{McG} (McGillis et al., 2001), which describes a gas transfer velocity controlled by breaking waves, is evaluated among

the various cubic wind speed dependencies published in the literature. The various expressions are as follows:

$$k_{\mathrm{L\&M}} = (aU_{10} + b)\left(\frac{Sc}{600}\right)^{-c}, \quad (2)$$

$$k_{\mathrm{W}} = 0.31U_{10}^2\left(\frac{Sc}{660}\right)^{-0.5}, \quad (3)$$

$$k_{\mathrm{N}} = (0.222U_{10}^2 + 0.333U_{10})\left(\frac{Sc}{600}\right)^{-0.5}, \quad (4)$$

$$k_{\mathrm{S}} = 0.27U_{10}^2\left(\frac{Sc}{660}\right)^{-0.5}, \quad (5)$$

$$k_{\mathrm{McG}} = (3.3 + 0.026U_{10}^3)\left(\frac{Sc}{660}\right)^{-0.5}, \quad (6)$$

where the coefficients a, b and c are dependent on the wind speed (see Liss and Merlivat, 1986), Sc refers to the Schmidt number and U_{10} is the wind speed at 10 m height. The various expressions are scaled to 600 or 660, which are the Sc values in fresh water or sea water, respectively, at a temperature of 20 °C.

2.3 Wind products

Wind products will be compared with observations (see Fig. 1) at the ocean buoys of Gascogne (45.20° N, 5.00° W) in the central part of the Bay of Biscay, owned and maintained by UK Met Office (http://www.metoffice.gov.uk/), and Silleiro (42.10° N, 9.39° W), Vilano (43.49° N, 9.21° W), Bares (44.06° N, 7.62° W), Peñas (43.73° N, 6.16° W) and Bilbao (43.63° N, 3.04° W), all of them supported by the Deep Water Network (Álvarez-Fanjul et al., 2003) of the Spanish institution Puertos del Estado (http://www.puertos.es). Hourly winds, averaged over 10 min intervals, are quality-checked by a simple statistical check, rejecting observations below the accuracy of the instrument ($\pm 0.3\,\mathrm{m\,s^{-1}}$) and outliers higher than 3σ from a 12 h running mean. The remaining data are height-adjusted to the equivalent 10 m winds following a logarithmic wind speed profile, which is defined for a neutral boundary

$$U_{(z)} = \frac{u_*}{\kappa}\ln\left(\frac{z}{z_0}\right) \quad (7)$$

where u_* is the friction velocity, κ the von Kármán constant (empirical value of 0.4), z the height over the sea level and z_0 is the aerodynamic roughness length. Using an initial roughness length for the sea surface, the 10 m winds and u_* are calculated following Vera (1983, unpublished manuscript and published as Eq. 8 in Large et al., 1995). The estimation is improved by an iterative procedure until an appropriate convergence criterion is reached (in this case until the difference between estimations of U_{10} is less than $0.001\,\mathrm{m\,s^{-1}}$). The effect of atmospheric stability in the comparisons between models and observations is of secondary importance, and anemometer measurements of 10 m winds are typically about $0.2\,\mathrm{m\,s^{-1}}$ lower than the equivalent neutral stability winds at 10 m (e.g., Chelton and Freilich, 2005; Sánchez et al., 2007). The availability of data during the study period is 98 % at Gascogne, 91 % at Peñas, 89 % at Silleiro, 73 % at Vilano and 29 % at Bilbao.

Wind data from the widely used NCEP/NCAR Reanalysis 1 (hereafter NCEP-1; Kalnay et al., 1996; Kanamitsu et al., 2000) and the NCEP/DOE Reanalysis 2 projects (hereafter NCEP-2; Kanamitsu et al., 2002) were selected as representatives of first generation reanalysis. Both datasets are maintained by the NOAA/OAR/ESRL PSD, Boulder, Colorado, USA, and provided through their Web site at http://www.cdc.noaa.gov/. In the second version, the planetary boundary layer non-local vertical diffusion scheme was implemented (Hong and Pan, 1996), more observations added, assimilation errors corrected, the orography smoothed and parameterizations of physical processes were updated – especially those concerning convection. Both datasets are obtained in a 1.875° spatial resolution T62 Gaussian grid with 6 h of temporal resolution. The only available and best guess for the 10 m wind speed within the reanalysis comes from the forecast time step, which is valid 6 h after the reference time.

ERA-Interim is the latest global atmospheric reanalysis produced by European Centre from Medium-Range Weather Forecasts (ECMWF). This project was conducted in part to replace ERA-40 (Uppala et al., 2005), in order to address several data assimilation problems encountered and to improve on various technical aspects of reanalysis such as data selection, quality control, bias correction and performance monitoring (Dee et al., 2011). Wind gridded data have a spatial T255 horizontal resolution, which corresponds to a spacing of approximately 79 km on a reduced Gaussian grid, and are produced with a temporal resolution of 6 h.

To include some of the various regional forecast models available in the Bay of Biscay, we have also analyzed winds from the HIRLAM model, running operationally at AEMet, Spain (http://www.aemet.es). Results used in this study come from a configuration run over Europe and the North Atlantic Ocean with 0.2° spatial and 6 h temporal resolution. Lateral open boundaries are forced with results of the global configuration of the ECMWF. Details on the physics of this model can be found in Undén et al. (2002).

In last years, winds derived under the Cross-Calibrated Multi-Platform (CCMP) project (Atlas et al., 2011) have become to be extensively used. Here, we have selected the L3.0 first-look analysis product, which combines satellite winds obtained from multiple remote sensing systems (SSM/I, SSMIS, AMSR-E, TRMM TMI, QuikSCAT, SeaWinds, WindSat and others) to produce a 6-hourly high-resolution (0.25°) cylindrical coordinate gridded analysis. A cross-calibrated sea-surface emissivity model function

improves the consistency between wind speed retrievals from microwave radiometers and those from scatterometers. The variational analysis method (VAM) combines these data with in situ measurements and a starting estimate (first guess) of the wind field, obtained during our study period from the ECMWF operational analysis.

Finally, Level 2B QuikSCAT winds have been obtained from the Center for Satellite Exploitation and Research (CERSAT) extraction service (http://www.ifremer.fr/cersat), which distributes the data of NASA PO.DAAC-JPL (Physical Oceanography Distributed Active Archive Center – Jet Propulsion Laboratory) as a mirror site for Europe. This processing level estimates winds with a 25×25 km resolution using the direction interval retrieval (DIR) algorithm that determines the most likely wind vector. Thus, the first screening is based on the JPL wind vector cell quality flag: cells with poor azimuth diversity, land contamination and derived winds outside the optimum modulus range were removed. Additionally, the Impact-based Multidimensional Histogram (IMUDH) (Huddleston and Stiles, 2000) was applied in heavy rain areas. After the JPL processing, an accuracy of the modulus of $\pm 2\,\mathrm{m\,s^{-1}}$ (independent of the wind speed in a range of 3–20 $\mathrm{m\,s^{-1}}$) and $\pm 20°$ in direction is obtained. Uncertainties related to higher and older wind waves, which may cause enhancing of backscattering under the same wind conditions in the range of 9–12 $\mathrm{m\,s^{-1}}$ (Ebuchi et al., 2002), were not considered.

3 Results and discussion

Figure 1 shows the problem associated with the selection of a specific wind product and its spatial and temporal interpolation to the position of the vessel taking underway ΔpCO_2 measurements during its first route. The wind speed clearly differs along the route from one product to another, with a noticeable bias exceeding 4.5 $\mathrm{m\,s^{-1}}$ among QuikSCAT and NCEP-2. These winds, in combination with the various expressions for k, will constitute the final ensemble of FCO_2 estimations that will be evaluated in the present study.

3.1 Comparison of ocean buoys and meteorological models

Which model performs better along the Bay of Biscay? Does this performance differ among different locations? To answer these questions the observed time series have been subsampled at 00:00, 06:00, 12:00 and 18:00 UTC in order to match the temporal resolution provided by the models, which have been interpolated to the location of the buoys.

With the previous criterion, Table 1 compares mean winds during the whole study year and during two periods mainly characterized by downwelling (when south–southwesterly wind events are dominant) and upwelling (north–northeasterly) conditions (October 2002–February 2003 and April 2003–August 2003, respectively; note that transition months between seasons have been discarded). The separation of the seasonal cycle was done in order to know the consistency of the wind speed (WS) products under both scenarios, which have a noticeable impact on the biogeochemical cycles, especially on the Iberian coast (Pérez et al., 2010).

Regarding the in situ observations, Silleiro is the location with the highest annual mean WS (7.06 $\mathrm{m\,s^{-1}}$) followed by the open ocean buoys of Gascogne and Vilano. Although Silleiro presents a high mean wind speed during both downwelling and upwelling periods, the highest mean value is achieved at Gascogne (8.60 $\mathrm{m\,s^{-1}}$) during the first season and at Vilano (6.93 $\mathrm{m\,s^{-1}}$) during the second one. Lower WS measurements for any period are found at the coastal enclosed buoys of Peñas and Bilbao.

With the exception of the Peñas buoy, which is the one closest to the coastline (16 km), NCEP-1 showed an underestimation of mean wind speed. This underestimation was especially intensified when data were constrained to the upwelling period. These results contrasted with the positive bias of NCEP-2, especially during the downwelling period, when it was up to 23 % higher. In the comparison at Peñas, both products overestimate winds, and in the case of NCEP-2 the positive bias is up to 45 % during the downwelling period.

The mean bias of NCEP-2 with respect to NCEP-1 was 1–1.6 $\mathrm{m\,s^{-1}}$, depending on the selected station, which is similar to the bias up to 2 $\mathrm{m\,s^{-1}}$ reported by Winterfeldt (2008) in the English Channel, and it is in accordance with other studies in different regions around the world (e.g., Jiang et al., 2005; Kubota et al., 2008). Here, both products had similar correlations (r) with the observations (< 0.6 at Peñas and Bilbao and ranging from 0.7 to 0.82 at the rest of the stations). The root mean square (rms) computations, with values ranging from 2.2 $\mathrm{m\,s^{-1}}$ in Gascogne to 3.0 $\mathrm{m\,s^{-1}}$ in Bilbao, were 0.4–0.7 $\mathrm{m\,s^{-1}}$ lower in NCEP-1. Nevertheless, this fact does not necessarily imply a worse comparison of NCEP-2 with observations from buoys in other regions since none of the reanalysis products are uniformly superior in all aspects, as reported by Jiang et al. (2005) in the equatorial Pacific Ocean and Winterfeldt (2008) in the English Channel.

In general terms, both the last generation reanalysis model ERA-Interim and the high-resolution forecast model HIRLAM-AEMet simulated the variability of the observed time series better than NCEP-1 and NCEP-2, and they did it better at the open ocean station of Gascogne than at the coastal stations of Bilbao and Peñas. However, the ensemble satellite observations of the CCMP product achieved the best results in terms of r (0.65 at Bilbao and > 0.8 at the rest of the stations) and rms (< 2.1 $\mathrm{m\,s^{-1}}$ in all stations). Whereas this product overestimated observed winds at all stations during the downwelling season, ERA-Interim underestimated them during the upwelling one.

The good performance of ERA-Interim in contrast to NCEP products may be related to its higher spatial

Table 1. Mean (and standard deviation) observed wind speeds and the mean difference (and standard deviation of the difference) of the models from observations during the complete study period (a), during the downwelling season, defined here from October to February (b) and the upwelling season, defined from April to August (c). The number of pairs compared at each buoy is shown in brackets. Units are $m\,s^{-1}$.

		Buoy	Differences with in situ observations				
			NCEP	NCEP2	HIRLAM	ERA-Interim	CCMP
(a) Annual	Silleiro (1301)	7.06 ± 3.71	-0.59 ± 0.14	1.04 ± 0.16	0.28 ± 0.15	-0.33 ± 0.14	-0.03 ± 0.14
	Vilano (1063)	6.82 ± 3.60	-0.89 ± 0.15	0.33 ± 0.16	-0.03 ± 0.16	0.04 ± 0.15	-0.09 ± 0.15
	Bares (906)	6.68 ± 3.47	-0.21 ± 0.16	1.22 ± 0.18	0.40 ± 0.18	0.09 ± 0.16	0.31 ± 0.16
	Peñas (1336)	5.61 ± 3.29	0.65 ± 0.13	2.17 ± 0.15	0.27 ± 0.13	0.03 ± 0.12	-0.02 ± 0.13
	Bilbao (429)	5.31 ± 2.70	-0.89 ± 0.17	0.11 ± 0.19	-0.40 ± 0.18	-1.27 ± 0.16	-1.17 ± 0.16
	Gascogne (1425)	6.98 ± 3.61	-0.04 ± 0.14	1.38 ± 0.16	-0.13 ± 0.14	-0.09 ± 0.14	0.01 ± 0.14
(b) Downwelling period	Silleiro (575)	8.19 ± 3.63	-0.53 ± 0.21	1.44 ± 0.25	0.21 ± 0.23	-0.19 ± 0.22	0.09 ± 0.22
	Vilano (219)	7.41 ± 3.77	-0.61 ± 0.36	0.78 ± 0.42	0.12 ± 0.39	0.20 ± 0.37	0.09 ± 0.36
	Bares (316)	7.63 ± 3.68	-0.02 ± 0.29	1.76 ± 0.35	0.60 ± 0.31	0.25 ± 0.29	0.53 ± 0.30
	Peñas (597)	6.64 ± 3.62	0.99 ± 0.21	3.00 ± 0.25	0.47 ± 0.22	0.38 ± 0.20	0.37 ± 0.20
	Bilbao (9)	–	–	–	–	–	–
	Gascogne (580)	8.60 ± 4.02	0.07 ± 0.24	2.04 ± 0.27	-0.02 ± 0.24	0.11 ± 0.23	0.17 ± 0.23
(c) Upwelling period	Silleiro (601)	6.39 ± 3.64	-0.78 ± 0.18	0.61 ± 0.20	0.34 ± 0.21	-0.46 ± 0.19	-0.09 ± 0.20
	Vilano (601)	6.93 ± 3.56	-1.17 ± 0.19	0.02 ± 0.21	-0.17 ± 0.21	-0.10 ± 0.20	-0.26 ± 0.19
	Bares (392)	6.17 ± 3.20	-0.25 ± 0.23	0.99 ± 0.25	0.15 ± 0.25	-0.03 ± 0.23	0.08 ± 0.23
	Peñas (592)	4.76 ± 2.69	0.38 ± 0.15	1.45 ± 0.17	0.05 ± 0.16	-0.29 ± 0.15	-0.40 ± 0.15
	Bilbao (285)	5.32 ± 2.73	-0.84 ± 0.21	0.04 ± 0.24	-0.42 ± 0.23	-1.21 ± 0.20	-1.18 ± 0.20
	Gascogne (602)	5.79 ± 2.71	-0.23 ± 0.16	0.71 ± 0.18	-0.36 ± 0.16	-0.41 ± 0.16	-0.19 ± 0.16

resolution, although the reduction of model biases is also dependent on model physics and configuration (e.g., Tinis et al., 2006; Otero and Ruiz-Villarreal, 2008). ERA-Interim is a step forward in global reanalysis models, and the contrast with NCEP products is evident. Thus, whereas NCEP-1 has substantial problems that limit its use, particularly for global climate change and variability studies (Trenberth et al., 2010), NCEP-2 is still a first generation reanalysis with an even worse performance in our study area.

The high-resolution HIRLAM-AEMet configuration did not perform as well as initially expected during the study period, with the exception of the results at Peñas. Better results are expected with subsequent improvements of the model configuration, which includes, among others, a short range ensemble prediction, 3DVAR assimilation scheme and the upgrade of physical parameterization (Yang, 2007). In the near-shore zone, where the wind drop-off does not seem to converge as model resolution increases (Capet et al., 2004), the improvement could be limited. Thus, different spatial resolutions in the same model will influence the estimation of CO_2 fluxes across these areas. Hence, further studies are required to gain insight into this aspect.

3.2 Observations from QuikSCAT

From the total of 1037 QuikSCAT satellite passes over the Bay of Biscay region during the study year, only 49 % had an observation over the Gascogne buoy, lowering the number of observations due to land contamination at Silleiro (27 %), Bares (4 %) and Vilano (3 %). The use of swath (Level 2B) and not gridded data (Level 3) implies that the preprocessing algorithm checks the center of the wind vector cell against the sea–land map. Thus, cells close to the coast will be or not land contaminated depending on the position of the cell and the resolution of the sea–land map in that region. Peñas and Bilbao – located ~ 21 km and ~ 16 km from the coast, respectively – were permanently out of the observed valid area of the scatterometer.

Mean satellite-retrieved wind speeds were higher than those observed at buoys (collocated data with a time criterion limit of 30 min; similar criterion to Pickett et al., 2003), ranging from a bias of $0.24\,m\,s^{-1}$ in Vilano to $0.60\,m\,s^{-1}$ in Silleiro (rms $< 1.5\,m\,s^{-1}$, $r > 0.9$ in all stations), performing even better (rms $< 1\,m\,s^{-1}$) when data were restricted to the upwelling season in Bares and Gascogne. These associated errors are in similar range as previous comparisons with buoys in other areas (e.g., Ebuchi et al., 2002; Pickett et al., 2003; Sánchez et al., 2007).

The inter-comparison of satellite (semidiurnal), model (6 hourly) and buoy winds demands a more restrictive criterion to limit synoptic scale differences. Satellite ascending passes between 05:30 and 06:30 UTC and descending between 17:30 and 18:30 UTC were selected to compare with coexisting model and observations at 00:00 and 18:00 UTC. This restrictive criterion reduces the dataset to

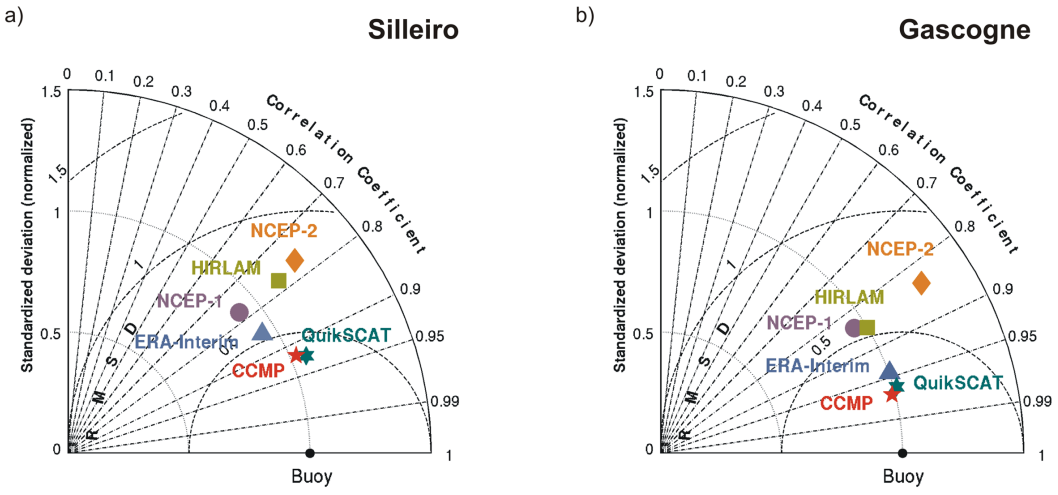

Fig. 2. Taylor diagrams showing the comparison of various wind products and anemometer winds at the Silleiro and Gascogne buoys. The diagram is constructed in terms of the correlation among time series, their centered root-mean-square (rms) difference and the standard deviation (σ) normalized by the amplitude of the observations.

111 observations at Silleiro and 230 at Gascogne and none at the other stations. With the exception of NCEP-2, the biases of the different wind products are lower at the ocean station of Gascogne than at the coastal station of Silleiro. QuikSCAT winds present, respectively to both stations, a mean bias of 0.17 and 0.64 m s^{-1}. Among the rest of the WS products, the smallest biases are achieved by NCEP-1 at Gascogne (-0.02 m s^{-1}) and CCMP at Silleiro (-0.20 m s^{-1}). Figure 2 summarizes the main statistics by using Taylor's diagram (Taylor, 2001), a useful tool in evaluating the relative skill of many different models. All wind products performed better at the open ocean station of Gascogne than at Silleiro; CCMP and QuikSCAT were the best products in statistical terms, closely followed by ERA-Interim, contrasting again with the higher amplitude and normalized rms difference of NCEP-2. CCMP is based on satellite-retrieved winds, which explains its high similarity with QuikSCAT. In this sense, the good performance of ERA-Interim is also related to the assimilation of scatterometer ocean surface winds, which includes data from QuikSCAT (aggregated at 50 km resolution), introduced in February 2000 until the end of 2009 (Dee et al., 2011).

Errors associated with the fact that satellite scatterometers retrieve winds relative to a moving sea surface (Kelly et al., 2001) are expected to be low, at least off western Iberia, as stated by the low speed ocean surface currents observed at the outer shelf buoy of Silleiro (0.14 ± 0.1 m s^{-1}). The bias with models may increase due to mesoscale fluctuations during weak wind events of the upwelling season, when diurnal breezes establish, or during atmospheric convective processes related to the influence of sea surface temperature (Austin and Pierson, 1999).

Finally, as a cautionary note on using QuikSCAT Level 3 gridded data instead of Level 2B, this product consists of separate maps for both the ascending and descending passes – to facilitate studies with diurnal trends – grouped in the same grid at nearly the original Level 2B sampling resolution. Consecutive satellite passes systematically overlap their swaths at latitudes higher than 48° N and, when this occurs, values are over-written, not averaged. However, at the latitude of the Cantabrian slope (44° N), a gap ($\sim 2°$ wide) between the swaths of two consecutive passes is formed with a 4-day frequency, avoiding sometimes the complete collocation of QuikSCAT winds along a route at these latitudes.

3.3 Wind speed, gas transfer velocity and CO_2 flux in the ECO route

How much does the selection of a specific wind product influence the estimation of the net sea–air FCO_2 in combination with different k parameterizations? Table 2 shows the mean FCO_2 computed using only the ECO routes with satellite data close in space (< 12.5 km) and time (< 3 h). This selection criterion (in the same way as the QuikSCAT subplot in Fig. 1), which was chosen to allow the use of all outputs of the meteorological model and to limit synoptic scale differences, retained 22 % of the original data. All results confirmed the role of the Bay of Biscay as a net CO_2 sink during the study period.

At this point and despite being usually omitted in the literature, it is important to mention that the expression of the gas transfer velocity depends on the specific wind speed field used during its computation – for example, k_S was originally estimated using global NCEP-1 winds. Thus, the use of a wind speed product different to the original one will produce a bias in k and, therefore, in the FCO_2 estimation. Naegler et al. (2006) dealt with this issue, and they normalized the gas transfer exchange to correct the biases of the wind fields at

Table 2. Mean (and standard deviation) of the FCO_2 flux (mmol m^{-2} day^{-1}) computed along the ECO route using various wind products and gas transfer velocity parameterizations, during the complete study period (a), during the downwelling season, defined here from October to February (b) and the upwelling season, defined from April to August (c).

		NCEP-1	NCEP-2	HIRLAM	ERA-Interim	CCMP	QuikSCAT
(a) Annual	$k_{L\&M}$	-1.24 ± 1.51	-1.74 ± 2.20	-1.40 ± 1.75	-1.31 ± 1.62	-1.35 ± 1.59	-1.43 ± 1.74
	k_N	-1.78 ± 2.12	-2.47 ± 3.07	-1.98 ± 2.42	-1.84 ± 1.31	-1.90 ± 2.19	-2.02 ± 2.41
	k_S	-1.90 ± 2.36	-2.70 ± 3.49	-2.14 ± 2.74	-1.98 ± 2.50	-2.04 ± 2.44	-2.18 ± 2.70
	k_W	-2.19 ± 2.71	-3.10 ± 4.01	-2.46 ± 3.14	-2.27 ± 2.87	-2.34 ± 2.80	-2.50 ± 3.10
	k_{McG}	-2.25 ± 3.06	-3.64 ± 5.54	-2.74 ± 4.17	-2.36 ± 3.95	-2.43 ± 3.28	-2.68 ± 3.85
(b) Downwelling period	$k_{L\&M}$	-1.39 ± 1.09	-1.98 ± 1.60	-1.71 ± 1.71	-1.43 ± 1.17	-1.54 ± 1.23	-1.63 ± 1.30
	k_N	-2.00 ± 1.50	-2.82 ± 2.19	-2.44 ± 2.36	-2.05 ± 1.60	-2.20 ± 1.68	-2.31 ± 1.78
	k_S	-2.16 ± 1.72	-3.11 ± 2.54	-2.67 ± 2.70	-2.21 ± 1.83	-2.38 ± 1.92	-2.51 ± 2.04
	k_W	-2.47 ± 1.97	-3.57 ± 2.92	-3.06 ± 3.11	-2.53 ± 2.10	-2.73 ± 2.21	-2.88 ± 2.35
	k_{McG}	-2.65 ± 2.41	-4.34 ± 4.37	-3.67 ± 4.75	-2.72 ± 2.67	-2.97 ± 2.85	-3.19 ± 3.12
(c) Upwelling period	$k_{L\&M}$	-1.09 ± 1.85	-1.50 ± 2.72	-1.13 ± 1.81	-1.17 ± 1.96	-1.11 ± 1.82	-1.16 ± 1.97
	k_N	-1.56 ± 2.63	-2.14 ± 3.81	-1.59 ± 2.52	-1.62 ± 2.72	-1.53 ± 2.50	-1.62 ± 2.72
	k_S	-1.67 ± 2.91	-2.34 ± 4.31	-1.71 ± 2.78	-1.73 ± 3.01	-1.63 ± 2.76	-1.74 ± 3.03
	k_W	-1.91 ± 3.34	-2.69 ± 4.95	-1.96 ± 3.20	-1.99 ± 3.46	-1.88 ± 3.17	-1.99 ± 3.48
	k_{McG}	-1.92 ± 3.67	-3.10 ± 6.64	-1.97 ± 3.55	-2.03 ± 4.03	-1.85 ± 3.58	-2.07 ± 4.26

global scale. However, the variability of the wind products at global scale differs from that described in the Bay of Biscay (Table 1). Such is the case that the use of the re-assessed gas scaling parameter of Wanninkhof's transfer velocity (Naegler et al., 2006; Park and Wanninkhof, 2012) would even increase the final discrepancies between the FCO_2 estimations among wind products: NCEP-1, QuikSCAT and CCMP products, the only ones that can be evaluated. For these reasons, we have decided to include all the combinations in Table 2 to put in relevance the bunch of different estimations that we could obtain if the last argument were not taken into account.

Estimations range from the lowest mean annual CO_2 uptake computed with the combination of NCEP-1 and $k_{L\&M}$, to the highest estimation computed using the pair NCEP-2 and k_{McG}, by a factor of ~ 3. The selection of k is more sensitivity than the choice of the wind product. If we focus on the most reliable estimations done with CCMP winds, the result using k_{McG} is 80 % higher than the lowest estimation with $k_{L\&M}$; the difference between the quadratic expressions of k_W and k_N is 23 %. On the other hand, if we select a specific k parameterization and we only vary the selection of the WS product, the estimations range from the lowest mean CO_2 uptake obtained with NCEP-1 to the largest value using NCEP-2. Excluding both NCEP products, differences with the cubic expression k_{McG} are < 14 % among the rest of the wind products.

At seasonal scale, Table 2 shows that the net CO_2 uptake was higher during the downwelling season than during the upwelling one, in part due to the high wind speeds that took place during this season (Table 1). However, the relative standard deviations of the FCO_2 are higher during the upwelling season, a fact that cannot be explained in terms of wind variability.

Thus, the importance of changing the k parameterization and the wind speed product must be put into perspective with respect to the spatial and temporal variability of ΔpCO_2. The distribution of underway ΔpCO_2 measurements in the Bay of Biscay gathered during ECO cruises from November 2002 to September 2003 is shown in Fig. 3a. A general CO_2 undersaturation of the surface waters in the Bay of Biscay was observed during the entire seasonal cycle that reached minimum ΔpCO_2 values during April and May related to biological activity. Only summer months showed a slight oversaturation because of the warming of the surface waters (Padin et al., 2008). This behavior contrasted with the ΔpCO_2 variability in the Loire estuary – which permanently exceeded the atmospheric pCO_2 values – reaching values up to 1200 µatm. The intensification of the dominant heterotrophic processes in the Loire plume extended this oversaturation area in the French continental shelf during autumn 2002 (de la Paz et al., 2010). However, surface waters of the Galician continental shelf were undersaturated, even during summertime, probably because of the prevalence of cold upwelled waters in the area.

Figure 3b represents the spatiotemporal distribution of the WS anomalies between NCEP-2 and ERA-Interim, which showed the worst and the best performance in the Bay of Biscay, respectively, of the evaluated reanalysis models. The intense overestimation of NCEP-2 winds was clearly observed during the winter (within the downwelling period of Table 1), especially at the end of February; the inner Bay of Biscay showed differences up to 9 m s^{-1}. In spite of the described

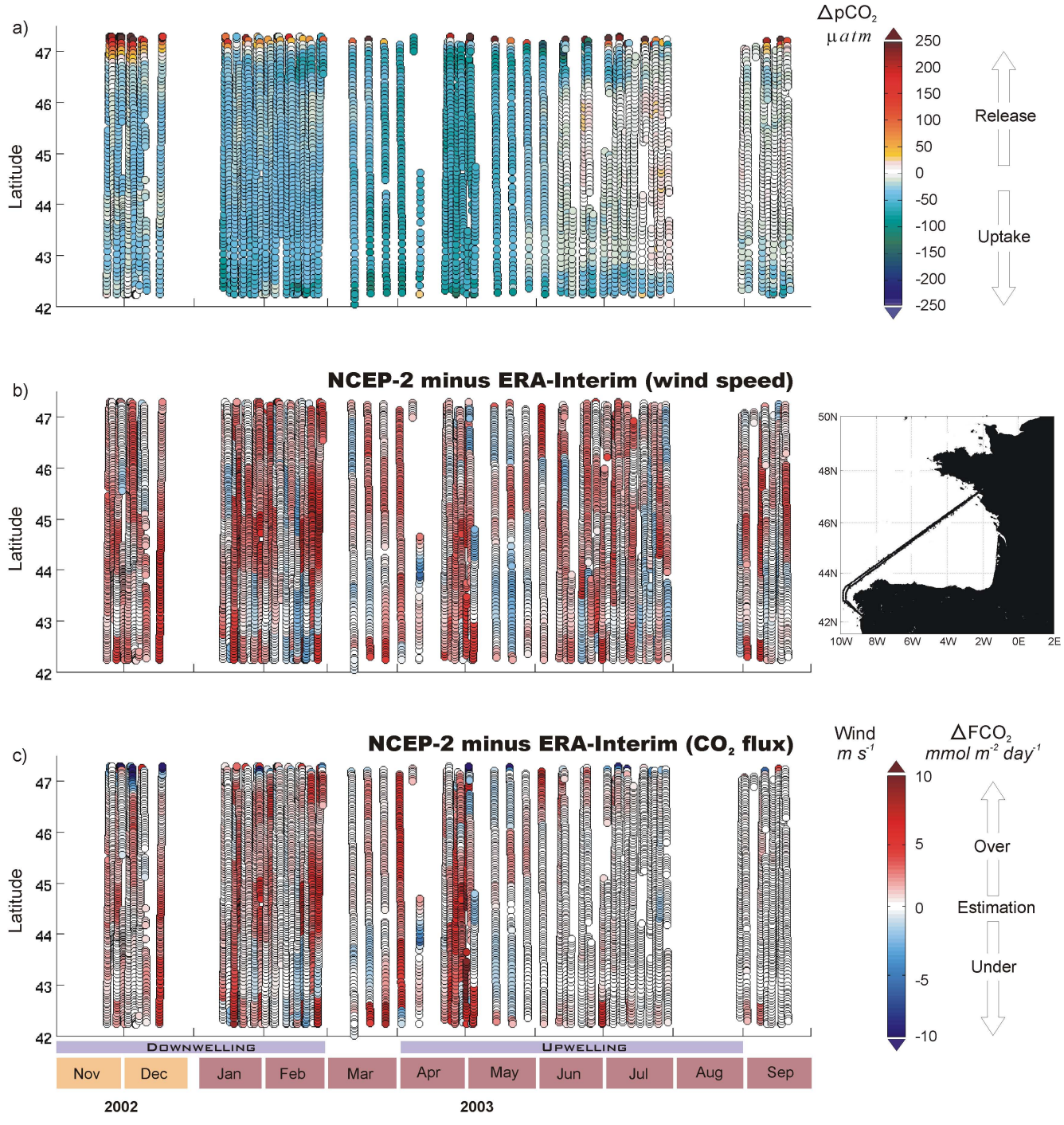

Fig. 3. (a) Distribution of underway ΔpCO_2 measurements in the Bay of Biscay gathered during ECO cruises. Positive (negative) means release (uptake). **(b)** Wind speed difference between NCEP-2 and ERA-Interim. **(c)** Difference of FCO_2 computed using NCEP-2 and ERA-Interim, both with the same algorithm by Wanninkhof (1992). Points along the route are drawn approximately each 30 min of navigation.

overestimation of the NCEP-2 wind fields, the difference was reverted in 31 % of the cases included in Fig. 3b.

By considering the most widely used parameterization k_W, FCO_2 anomalies along ECO cruises were estimated from NCEP-2 and ERA-Interim winds (Fig. 3c). The main FCO_2 differences were observed during the intense spring uptake (end of April and in the beginning of May) because of the intense CO_2 undersaturation (Fig. 3a) and the notable overestimation of NCEP-2 winds (Fig. 3b). These strong differences contrast with the maximum agreement from June to

September, with the exception of a particular route in the Galician shelf, when wind speed differed between both models. On the other hand, the behavior as a CO_2 source of the Loire plume ($> 46.5°$ N), with the exception of short periods of CO_2 absorption, was also overestimated during the maximum ΔpCO_2 events (see first fortnight of December and May) when NCEP-2 was used in comparison with ERA-Interim. Although these noticeable FCO_2 differences came from strong sea–air CO_2 disequilibrium, the WS disagreement between both models also had a significant impact on the FCO_2 values such as it was observed at the end of February. These differences are resumed in a higher CO_2 uptake using NCEP-2 ($-2.60 \pm 9.56\,\mathrm{mmol\,m^{-2}\,day^{-1}}$) than using ERA-Interim ($-1.82 \pm 7.77\,\mathrm{mmol\,m^{-2}\,day^{-1}}$).

The relative contribution to the FCO_2 variability of both k and ΔpCO_2 can be quantified as the equivalent standard deviation of the ΔpCO_2 that will cause as much standard deviation in fluxes as the variability of k (see Eq. 8 in Olsen et al., 2005). Subsequently, this value was compared with the in situ ΔpCO_2 variability; if the equivalent standard deviation of the ΔpCO_2 is higher than the in situ value, then the contribution of k to FCO_2 variability is higher than ΔpCO_2. The annual mean estimation done along the ECO routes shows that the k variability was always dominant with independence of the wind product and, obviously, in a ratio proportional to the dependence of k on wind speed (data not shown). This dominance is even higher when the estimation is restricted to the downwelling season, when strong southerly and southwesterly winds dominate associated with the passage of atmospheric fronts coming from the Atlantic. As an example, and using k_W and the reliable wind speed from CCMP, the ratio between the equivalent and the observed ΔpCO_2 variability was 1.15 during the whole study period, which contrasts with the 2.03 value when the data were restricted to the downwelling season. It is important to note that part of this dominance is highlighted by the overestimation that some wind products experiment during this period, as mentioned in Sect. 3.1. Unlike the downwelling season, ΔpCO_2 was the driving force of the FCO_2 variability during the upwelling one (in the example shown, the ratio lowered to 0.76).

Moreover, the relative contributions of both the wind speed and CO_2 saturation to FCO_2 variability are also dependent in the coastal area. Thus, k has a higher relative contribution than ΔpCO_2 at annual and seasonal scales off NW Iberia ($< 44°$ N), and consequently the selection of the wind product highly influences the FCO_2 variability in this area, where the change in the coastline orientation and the spatial resolution of models hamper the performance of the wind field. On the other hand, ΔpCO_2 drives the FCO_2 variability during the upwelling season in the coastal area off France ($> 46.5°$ N), in a region affected by the Loire estuary.

Finally, and reintroducing the initial question in this section, an applet was built using Processing (http://www.processing.org). This applet can be found at http://www.indicedeafloramiento.ieo.es/eco and allows exploring the spatiotemporal variability of air–sea CO_2 flux in our dataset.

4 Conclusions

In this paper, we have studied the uncertainties of the gas transfer velocity in a coastal region and their impact on the estimation of sea–air CO_2 fluxes. The results presented above show that the annual mean CO_2 uptake estimated in the Bay of Biscay may differ by up to a factor of ~ 3, depending on the wind speed product and the gas exchange parameterization used, where up to $\sim 110\,\%$ of the uncertainty is directly related to the selection of k and up to $\sim 62\,\%$ to the selection of the wind product. However, their differences could be maximized in specific regions and periods or during certain meteorological events, as stated by Otero and Ruiz-Villarreal (2008), who proved that getting similar mean values from different meteorological models does not necessarily imply an adequate description of temporal and spatial variations. So, with the exception of the upwelling season off the Loire estuary, the impact of the variability of the wind speed field in the FCO_2 estimation is higher than the observed ΔpCO_2 variability. Therefore, the community of CO_2 researchers and biogeochemistry modelers in coastal regions should be aware of the inherent uncertainties of the employed wind speed field and their variability because of the large impact on their results.

In the absence of in situ observations at buoys, QuikSCAT Level 2B data are a good choice to estimate FCO_2. However, land-contaminated regions preclude its use over coastal regions, and, in these situations, the use of reanalysis and forecast meteorological models is the best choice. In that case, NCEP-2 overestimates winds in the Bay of Biscay region, and although this pattern can revert during certain periods – especially during upwelling events – this product should not be considered for further FCO_2 studies, at least, with the current model configuration. The opposite effect is observed when using NCEP-1. Consequently, ERA-Interim – mainly due to its higher spatial resolution and the assimilation of scatterometer ocean surface winds – becomes a balanced choice among reanalysis models. A better solution is obtained from CCMP, which combines satellite-retrieved winds in an optimum way. Even though the HIRLAM-AEMet configuration shown in this study did not achieve optimum results, recent advances in data assimilation and computing capabilities should convert the use of limited area models in the preferred choice. In fact, strong updates in the current configuration have been performed by AEMet since the study period (Yang, 2007), which encourages using models from national or regional agencies.

Acknowledgements. We would like to thank the captains and crew of RORO *L'Audace* and RORO *Surprise*, and the management team from the Suardíaz Company, for their hospitality and essential

help throughout the sampling period. Many thanks to MeteoFrance, who provided the meteorological data from the Gascogne buoy. This work was developed and funded by the ECO project (MCyT REN2002-00503/MAR) and EU FP7 project CARBOCHANGE "Changes in carbon uptake and emissions by oceans in a changing climate" under agreement no 264879. Part of the wind analysis was performed in the framework of projects REFORZA (Xunta de Galicia, PGIDIT06RMA60401PR) and COVACLAN (Ministerio de Ciencia e Innovación, CTM-2007-64600/MAR). Pablo Otero is supported by "Observatorio oceánico del Margen Ibérico y del Litoral" (RAIA.co, POCTEP 2007-20130520_RAIA_CO_1_E).

Edited by: S. W. A. Naqvi

References

Álvarez-Fanjul, E., Alfonso, M., Ruiz, M. I., López, J. D., and Rodríguez, I.: Real time monitoring of Spanish coastal waters: The deep water network, Elsev. Oceanogr. Serie., 69, 398–402, 2003.

Atlas, R., Hoffman, R. N., Ardizzone, J., Leidner, S. M., Jusem, J. C., Smith, D. K., and Gombos, D.: A cross-calibrated, multiplatform ocean surface wind velocity product for meteorological and oceanographic applications, B. Am. Meteorol. Soc., 92, 157–174, doi:10.1175/2010BAMS2946.1, 2011.

Austin, S. and Pierson, W. J.: Mesoscale and synoptic-scale effects on the validation of NSCAT winds by means of data buoy reports, J. Geophys. Res.-Oceans, 104, 11437–11447, 1999.

Borges, A. V. and Frankignoulle, M.: Distribution of surface carbon dioxide and air-sea exchange in the upwelling system off the Galician coast, Global Biogeochem. Cy., 16, 13-1–13-13, doi:10.1029/2000GB001385, 2002.

Boutin, J., Etcheto, J., Merlivat, L., and Rangama, Y.: Influence of gas exchange coefficient parameterisation on seasonal and regional variability of CO_2 air-sea fluxes, Geophys. Res. Lett., 29, 23-1–23-4, doi:10.1029/2001GL013872, 2002.

Broecker, W. S., Peng, T.-H., Ostlund, G., and Stuiver, M.: The distribution of bomb radiocarbon in the ocean, J. Geophys. Res.-Oceans, 90, 6953–6970, doi:10.1029/JC090iC04p06953, 1985.

Capet, X. J., Marchesiello, P., and McWilliams, J. C.: Upwelling response to coastal wind profiles, Geophys. Res. Lett., 31, L13311, doi:10.1029/2004gl020123, 2004.

Chelton, D. B. and Freilich, M. H.: Scatterometer-based assessment of 10 m wind analyses from the operational ECMWF and NCEP numerical weather prediction models, Mon. Weather Rev., 133, 409–429, 2005.

Chelton, D. B. and Wentz, F. J.: Global microwave satellite observations of sea surface temperature for numerical weather prediction and climate research, B. Am. Meteorol. Soc., 86, 1097–1115, 2005.

Chen, C. T. A. and Borges, A. V.: Reconciling opposing views on carbon cycling in the coastal ocean: Continental shelves as sinks and near-shore ecosystems as sources of atmospheric CO_2, Deep-Sea Res. Pt. II, 56, 578–590, 2009.

Dee, D. P., Uppala, S. M., Simmons, A. J., Berrisford, P., Poli, P., Kobayashi, S., Andrae, U., Balmaseda, M. A., Balsamo, G., Bauer, P., Bechtold, P., Beljaars, A. C. M., van de Berg, L., Bidlot, J., Bormann, N., Delsol, C., Dragani, R., Fuentes, M., Geer, A. J., Haimberger, L., Healy, S. B., Hersbach, H., Holm, E. V., Isaksen, L., Kallberg, P., Kohler, M., Matricardi, M., McNally, A. P., Monge-Sanz, B. M., Morcrette, J. J., Park, B. K., Peubey, C., de Rosnay, P., Tavolato, C., Thepaut, J. N., and Vitart, F.: The ERA-Interim reanalysis: configuration and performance of the data assimilation system, Q. J. Roy. Meteor. Soc., 137, 553–597, 2011.

de la Paz, M., Padin, X. A., Ríos, A. F., and Pérez, F. F.: Surface fCO_2 variability in the Loire plume and adjacent shelf waters: High spatio-temporal resolution study using ships of opportunity, Mar. Chem., 118, 108–118, 2010.

DOE: Handbook of methods for the analysis of the various parameters of the carbon dioxide system in sea water, Version 2., edited by: Dickson, A. G. and Goyet, C., ORNL/CDIAC-74, 1994.

Ebuchi, N., Graber, H. C., and Caruso, M. J.: Evaluation of wind vectors observed by QuikSCAT/SeaWinds using ocean buoy data, J. Atmos. Ocean. Tech., 19, 2049–2062, 2002.

Erickson, D. J.: A stability dependent theory for air-sea gas-exchange, J. Geophys. Res.-Oceans, 98, 8471–8488, 1993.

Griessbaum, F., Moat, B. I., Narita, Y., Yelland, M. J., Klemm, O., and Uematsu, M.: Uncertainties in wind speed dependent CO_2 transfer velocities due to airflow distortion at anemometer sites on ships, Atmos. Chem. Phys., 10, 5123–5133, doi:10.5194/acp-10-5123-2010, 2010.

Gruber, N.: Anthropogenic CO_2 in the Atlantic Ocean, Global Biogeochem. Cy., 12, 165–191, 1998.

Hong, S. Y. and Pan, H. L.: Nonlocal boundary layer vertical diffusion in a Medium-Range Forecast Model, Mon. Weather Rev., 124, 2322–2339, 1996.

Huddleston, J. N. and Stiles, B. W.: A multidimensional histogram rain-flagging technique for SeaWinds on QuikSCAT, in: Proceedings IEEE 2000 International Geoscience and Remote Sensing Symposium (IGARSS), Vol I–VI, IEEE, New York, 1232–1234, 2000.

Jiang, C. L., Cronin, M. F., Kelly, K. A., and Thompson, L.: Evaluation of a hybrid satellite- and NWP-based turbulent heat flux product using Tropical Atmosphere-Ocean (TAO) buoys, J. Geophys. Res.-Oceans, 110, C09007, doi:10.1029/2004JC002824, 2005.

Kalnay, E., Kanamitsu, M., Kistler, R., Collins, W., Deaven, D., Gandin, L., Iredell, M., Saha, S., White, G., Woollen, J., Zhu, Y., Chelliah, M., Ebisuzaki, W., Higgins, W., Janowiak, J., Mo, K. C., Ropelewski, C., Wang, J., Leetmaa, A., Reynolds, R., Jenne, R., and Joseph, D.: The NCEP/NCAR 40-year reanalysis project, B. Amer. Meteorol. Soc., 77, 437–471, 1996.

Kanamitsu, M., Ebisuzaki, W., Woolen, J., Potter, J., and Fiorion, M.: An overview of NCEP/DOE Reanalysis-2, Second International Conference on Reanalyses, 2000.

Kanamitsu, M., Ebisuzaki, W., Woollen, J., Yang, S. K., Hnilo, J. J., Fiorino, M., and Potter, G. L.: NCEP-DOE AMIP-II reanalysis (R-2), B. Amer. Meteorol. Soc., 83, 1631–1643, 2002.

Kelly, K. A., Dickinson, S., McPhaden, M. J., and Johnson, G. C.: Ocean currents evident in satellite wind data, Geophys. Res. Lett., 28, 2469–2472, 2001.

Kubota, M., Iwabe, N., Cronin, M. F., and Tomita, H.: Surface heat fluxes from the NCEP/NCAR and NCEP/DOE reanalyses at the Kuroshio Extension Observatory buoy site, J. Geophys. Res.-Oceans, 113, C02009, doi:10.1029/2007JC004338, 2008.

Large, W. G., Morzel, J., and Crawford, G. B.: Accounting for surface-wave distortion of the marine wind-profile in low-level

ocean storms wind measurements, J. Phys. Oceanogr., 25, 2959–2971, 1995.

Laruelle, G. G., Durr, H. H., Slomp, C. P., and Borges, A. V.: Evaluation of sinks and sources of CO_2 in the global coastal ocean using a spatially-explicit typology of estuaries and continental shelves, Geophys. Res. Lett., 37, L15607, doi:10.1029/2010GL043691, 2010.

Liss, P. S. and Merlivat, L.: Air–sea gas exchange rates: introduction and synthesis, in: The role of air-sea exchange in geochemical cycling, D. Reidel Publishing Company, 113–127, 1986.

McGillis, W. R., Edson, J. B., Ware, J. D., Dacey, J. W. H., Hare, J. E., Fairall, C. W., and Wanninkhof, R.: Carbon dioxide flux techniques performed during GasEx-98, Mar. Chem., 75, 267–280, 2001.

Naegler, T., Ciais, P., Rodgers, K., and Levin, I.: Excess radiocarbon constraints on air-sea gas exchange and the uptake of CO_2 by the oceans, Geophys. Res. Lett., 33, L11802, doi:10.1029/2005gl025408, 2006.

Nightingale, P. D., Malin, G., Law, C. S., Watson, A. J., Liss, P. S., Liddicoat, M. I., Boutin, J., and Upstill-Goddard, R. C.: In situ evaluation of air-sea gas exchange parameterizations using novel conservative and volatile tracers, Global Biogeochem. Cy., 14, 373–387, doi:10.1029/1999gb900091, 2000.

Olsen, A., Wanninkhof, R., Trinanes, J. A., and Johannessen, T.: The effect of wind speed products and wind speed-gas exchange relationships on interannual variability of the air-sea CO_2 gas transfer velocity, Tellus B, 57, 95–106, 2005.

Otero, P. and Ruiz-Villarreal, M.: Wind forcing of the coastal circulation off north and northwest Iberia: Comparison of atmospheric models, J. Geophys. Res.-Oceans, 113, C10019, doi:10.1029/2008JC004740, 2008.

Padin, X. A., Vázquez-Rodríguez, M., Ríos, A. F., and Pérez, F. F.: Atmospheric CO_2 measurements and error analysis on seasonal air-sea CO_2 fluxes in the Bay of Biscay, J. Marine Syst., 66, 285–296, 2007.

Padin, X. A., Castro, C. G., Ríos, A. F., and Pérez, F. F.: fCO_{2SW} variability in the Bay of Biscay during ECO cruises, Cont. Shelf Res., 28, 904–914, 2008.

Park, G.-H. and Wanninkhof, R.: A large increase of the CO_2 sink in the western tropical North Atlantic from 2002 to 2009, J. Geophys. Res.-Oceans, 117, C08029, doi:10.1029/2011jc007803, 2012.

Pérez, F. F., Ríos, A. F., and Rosón, G.: Sea surface carbon dioxide off the Iberian Peninsula (North Eastern Atlantic Ocean), J. Marine Syst., 19, 27–46, 1999.

Pérez, F. F., Padin, X. A., Pazos, Y., Gilcoto, M., Cabanas, M., Pardo, P. C., Doval, M. D., and Farina-Busto, L.: Plankton response to weakening of the Iberian coastal upwelling, Glob. Change Biol., 16, 1258–1267, 2010.

Pickett, Mark, H., Wenqing, T., Rosenfeld, Leslie, K., Wash, and Carlyle, H.: QuikSCAT satellite comparisons with nearshore buoy wind data off the U.S. West Coast, American Meteorological Society, Boston, MA, ETATS-UNIS, 11 pp., 2003.

Riebesell, U., Kortzinger, A., and Oschlies, A.: Sensitivities of marine carbon fluxes to ocean change, P. Natl. Acad. Sci. USA, 106, 20602–20609, 2009.

Sabine, C. L., Feely, R. A., Gruber, N., Key, R. M., Lee, K., Bullister, J. L., Wanninkhof, R., Wong, C. S., Wallace, D. W. R., Tilbrook, B., Millero, F. J., Peng, T. H., Kozyr, A., Ono, T., and Ríos, A. F.: The oceanic sink for anthropogenic CO_2, Science, 305, 367–371, 2004.

Sánchez, R. F., Relvas, P., and Pires, H. O.: Comparisons of ocean scatterometer and anemometer winds off the southwestern Iberian Peninsula, Cont. Shelf Res., 27, 155–175, 2007.

Solomon, S., Qin, D., Manning, M., Alley, R. B., Berntsen, T., Bindoff, N. L., Chen, Z., Chidthaisong, A., Gregory, J. M., Hegerl, G. C., Heimann, M., Hewitson, B., Hoskins, B. J., Joos, F., Jouzel, J., Kattsov, V., Lohmann, U., Matsuno, T., Molina, M., Nicholls, N., Overpeck, J., Raga, G., Ramaswamy, V., Ren, J., Rusticucci, M., Somerville, R., Stocker, T. F., Whetton, P., Wood, R. A., and Wratt, D.: Contribution of Working Group I to the Fourth assessment report of the Intergovernmental Panel on Climate Change, Cambridge University Press, Cambridge, UK and New York, NY, USA, 996, 2007.

Sweeney, C., Gloor, E. M., Jacobson, A. R., Key, R. M., Galen, M., Sarmiento, J. F., and Wanninkhof, R.: Constraining Global air-sea Gas Exchange for CO_2 with recent Bomb ^{14}C measurements, Global Biogeochem. Cy., 21, GB2015, doi:10.1029/2006GB002784, 2007.

Takagaki, N. and Komori, S.: Effects of rainfall on mass transfer across the air-water interface, J. Geophys. Res.-Oceans, 112, C06006, doi:10.1029/2006JC003752, 2007.

Takahashi, T., Olafsson, J., Goddard, J. G., Chipman, D. W., and Sutherland, S. C.: Seasonal variation of CO_2 and nutrients in the high-latitude surface oceans: A comparative study, Global Biogeochem. Cy., 7, 843–878, doi:10.1029/93gb02263, 1993.

Takahashi, T., Sutherland, S. C., Wanninkhof, R., Sweeney, C., Feely, R. A., Chipman, D. W., Hales, B., Friederich, G., Chavez, F., Sabine, C., Watson, A., Bakker, D. C. E., Schuster, U., Metzl, N., Yoshikawa-Inoue, H., Ishii, M., Midorikawa, T., Nojiri, Y., Kortzinger, A., Steinhoff, T., Hoppema, M., Olafsson, J., Arnarson, T. S., Tilbrook, B., Johannessen, T., Olsen, A., Bellerby, R., Wong, C. S., Delille, B., Bates, N. R., and de Baar, H. J. W.: Climatological mean and decadal change in surface ocean pCO_2, and net sea–air CO_2 flux over the global oceans, Deep-Sea Res. Pt. II, 56, 554–577, 2009.

Taylor, K. E.: Summarizing multiple aspects of model performance in a single diagram, J. Geophys. Res.-Atmos., 106, 7183–7192, doi:10.1029/2000jd900719, 2001.

Tinis, S. W., Thomson, R. E., Mass, C. F., and Hickey, B. M.: Comparison of MM5 and meteorological buoy winds from British Columbia to northern California, Atmos. Ocean, 44, 65–81, 2006.

Trenberth, K. E., Dole, R., Xue, Y., Onogi, K., Dee, D., Balmaseda, M., Bosilovich, M., Schubert, S., and Large, W.: Atmospheric reanalyses: A major resource for ocean product development and modeling, OceanObs'09: Sustained Ocean Observations and Information for Society, Venice, Italy, 21–25 September 2009, 2010,

Tsai, W. T. and Liu, K. K.: An assessment of the effect of sea surface surfactant on global atmosphere-ocean CO_2 flux, J. Geophys. Res.-Oceans, 108, 3127, doi:10.1029/2000JC000740, 2003.

Undén, P., Rontu, L., Järvinen, H., Lynch, P., Calvo, J., Cats, G., Cuxart, J., Eerola, K., Fortelius, C., Garcia-Moya, J., Jones, C., Lenderlink, G., McDonald, A., McGrath, R., Navascues, B., Nielsen, N., Odegaard, V., Rodriguez, E., Rummukainen, M., Rõõm, R., Sattler, K., Sass, B., Savijärvi, H., Schreur, B., Sigg, R., The, H., and Tijm, A.: HIRLAM-5 Scientific Documentation,

Swedish Meteorological and Hydrological Institute, 2002.

Uppala, S. M., Kallberg, P. W., Simmons, A. J., Andrae, U., Bechtold, V. D., Fiorino, M., Gibson, J. K., Haseler, J., Hernandez, A., Kelly, G. A., Li, X., Onogi, K., Saarinen, S., Sokka, N., Allan, R. P., Andersson, E., Arpe, K., Balmaseda, M. A., Beljaars, A. C. M., Van De Berg, L., Bidlot, J., Bormann, N., Caires, S., Chevallier, F., Dethof, A., Dragosavac, M., Fisher, M., Fuentes, M., Hagemann, S., Holm, E., Hoskins, B. J., Isaksen, L., Janssen, P., Jenne, R., McNally, A. P., Mahfouf, J. F., Morcrette, J. J., Rayner, N. A., Saunders, R. W., Simon, P., Sterl, A., Trenberth, K. E., Untch, A., Vasiljevic, D., Viterbo, P., and Woollen, J.: The ERA-40 re-analysis, Q. J. Roy. Meteor. Soc., 131, 2961–3012, 2005.

Wanninkhof, R.: Relationship between wind speed and gas exchange over the ocean, J. Geophys. Res.-Oceans, 97, 7373–7382, doi:10.1029/92jc00188, 1992.

Weiss, R. F.: Carbon dioxide in water and seawater: the solubility of non-ideal gas, Mar. Chem., 2, 221–231, 1974.

Winterfeldt, J.: Comparison of measured and simulated wind speed data in the North Atlantic, GKSS-Forschungszentrum Geesthacht GmbH, Department Geowissenschaften der Universität Hamburg, 2008.

Yang, X.: Progress Report of the Operational HIRLAM, 70–76, 2007.